Non-Sweep Gas Pyrolysis with Vapor Heater using “Shorea Pinanga” as a feedstock

Nasruddin A. Abdullah
Heat Transfer Laboratory, Department of Mechanical Engineering Universitas Indonesia

Rachmat Rahardian
Heat Transfer Laboratory, Department of Mechanical Engineering Universitas Indonesia

Imansyah Ibnu Hakim
Heat Transfer Laboratory, Department of Mechanical Engineering Universitas Indonesia

Nandy Putra
Heat Transfer Laboratory, Department of Mechanical Engineering Universitas Indonesia

他

https://doi.org/10.5109/4150506

出版情報：Evergreen. 7 (4), pp.555-563, 2020-12. 九州大学グリーンテクノロジー研究教育センター
バージョン：

EVERGREEN Joint Journal of Novel Carbon Resource Sciences & Green Asia Strategy, Vol. 07, Issue 04, pp555-563, December 2020

Non-Sweep Gas Pyrolysis with Vapor Heater using "Shorea Pinanga" as a feedstock

Nasruddin A. Abdullah[1,2,*], Rachmat Rahardian[1], Imansyah Ibnu Hakim[1], Nandy Putra[1,*], Raldi A. Koestoer[1]
[1]Heat Transfer Laboratory, Department of Mechanical Engineering Universitas Indonesia, Kampus UI Depok 16424, Indonesia
[2]Department of Mechanical Engineering, Faculty of Engineering Universitas Samudra, Kota Langsa, 24416, Indonesia

*Author to whom correspondence should be addressed:
E-mail:nandyputra@eng.ui.ac.id; nasruddin@unsam.ac.id

(Received November 4, 2020; Revised December 9, 2020; accepted December 16, 2020).

Abstract: Biomass is abundant and sustainable with CO2 neutral and less dependent on climate. Its potential application could be obtained from biomass by the pyrolysis process. Meranti sawdust from industrial waste is widely available and can be used as feedstock to produce bio-oil through the pyrolysis process. The utilization of nitrogen as a sweep gas in pyrolysis requires additional components and incurs additional costs in production. The research aims to investigate non-sweep gas pyrolysis with vapor heater using Meranti (Shorea pinanga) as feedstock. The Proportional Integral Differential (PID) was installed to control the reactor and reaction zone temperature. Liquid yield increased due to the increased surface temperature at the reaction zone. The maximum liquid yield was obtained of 39 wt% at the reaction zone temperature 150 ºC. The liquid yield composition consists of a high boiling substance with a higher heating value and an increase of vapor temperature. Meanwhile, the liquid product without a heater in the reaction zone relatively contained the compound with a lower boiling point, and it had a lower heating value.

Keywords: liquid yield; meranti wood; pyrolysis; reaction zone; vapor temperature

1. Introduction and background

The availability of biomass is abundant and sustainable with CO2 neutral and less dependent on climate [1]. Besides massive energy consumption [2], including the total energy use by building [3], biomass waste's burning contributes to global emission [4].

Various types of biomass have been used for the feedstock in the pyrolysis process, such as the waste of agriculture crops [5], palm fiber [6], pine [7][8], oak [9], cotton cocoon shell [10][11], and sawdust [12][13]. Meranti is one type of wood that is easy to get in Indonesia, and the wood used is from industry and forestry waste. Pyrolysis is the decomposition process by heating without involving oxygen and knows as the thermochemical decomposition process to convert organic material into the volatile matter, and the remaining substance is converted into the rich solid of carbon [14][15]. The liquid was produced from this process, known as bio-oil. This liquid can be applied as a preservative, fuel, and other chemical substances [16][17]. The type and composition of biomass affect the composition of bio-oil [1].

Meranti was used as feedstock using fixed bed and nitrogen as a sweep gas to condense pyrolysis vapor using ethylene glycol below –10 ºC[18] and equipped with reactor temperature controller [19].

Pyrolysis is the best way to convert solid biomass into a liquid, and carbonization activation is an effective process to produce char and gas [20]. The volatile matter produced in the reactor consist of condensable and non-condensable (NCG) vapor. The condensable vapor was condensed into the liquid collection system (LCS) to be a liquid form. The application of the bio-oil dependent on the composition of its content. The process and raw material also influence the compositions of the liquid yield. The raw material for feedstock is the main component of the pyrolysis to get a particular compound. Besides that, moisture content, reaction temperature, heating rate, sweeping gas flow rate, resident time, and cooling temperature are the parameters that influenced the product of pyrolysis. Those variables are the operating parameters to determine the composition and the liquid yield of the pyrolysis process. The compound of vapor generated by reactors consists of many boiling fraction temperatures; high, middle, and low boiling points. The high boiling point results in the liquid with a high heating value, vice versa, low boiling point. The high boiling point results in the liquid with a high heating value, vice versa, low boiling point fraction produces more acidity and low heating value [21] .

The pyrolysis process produces an amount of pyrolysis vapor in the pyrolysis reactor. The vapor encounters a secondary reaction in the reaction zone and reduces in liquid yield [22][23] . The reaction zone is the area where the vapor is accumulation before entering the condensation zone. The vapor temperature in the reaction zone was influenced by the heating rate and pyrolysis temperature. The vapor pressure in the reaction zone was relatively low, and the vapor temperature was around 110 ℃ [24] . Schulzke at el., installed electrical trace heating at the reaction zone's piping line to avoid the vapor condensation before LCS [21] . This heater also affects the pyrolysis product and pyrolysis process.

The vapor heater was installed to maintain vapor temperature constantly and avoid vapor condensed at the reaction zone area. Non-sweep gas pyrolysis is a pyrolysis process without involving the carrier gas to sweep pyrolysis vapor from the reaction zone to the condensation zone. Supramono et.al. obtained the higher liquid and the lower yield of char by a higher gas flow rate of N_2 [25] . CO2 as carrier gas has been implemented in pyrolysis, the product yield increases compared to the use of N2 for pyrolysis and lower yield for co-pyrolysis [26] . The use of carrier gas incurs additional cost and additional energy, and it needs more supporting equipment. Therefore, the non-sweep gas reactor needs a comprehensive study regarding the optimum liquid yield, thermal characteristics, and liquid yield properties.

This paper presents the investigation of non-sweep gas pyrolysis with vapor heater using *Meranti (Shorea pinanga)* as feedstock.

2. Methods and experimental setup

2.1 Materials and preparation

Meranti wood (*Shorea pinanga*) from industrial waste was used as feedstock. The raw materials were treated with two treatments, thermal and physical. The physical treatment, including crushing and grinding the raw materials into 25 mesh (700 μm). Simultaneously, the thermal treatment was drying the raw materials at 80 ºC in the vacuum drying for 4 hours to vaporize water vapor and reduce water content below 10-wt%. The raw material was weighed before feeding into the reactor. Moisture content below 10 wt% is recommended and suitable for the pyrolysis process to produce bio-oil [27] . Moisture content affects the liquid oil properties such as pH, heating value, and viscosity [28] . The total weight of feedstock was 200 grams with a density of 332.9 kg/m³.

2.2 Tubular fixed-bed reactor and condenser

The decomposition process was performed in a tubular fixed-bed reactor, sized 3” in diameter, Schedule 10S, and 270-mm height. The fixed-bed reactor equipped with an electric heater was controlled by a proportional integral and differential (PID) controller. There was not any carrier gas flows in the reactor. The pyrolysis vapor flowed naturally. The pyrolysis vapor was generated in the reactor and accumulated in the reaction zone. The vapor heater was equipped at the reaction zone to keep the vapor temperature at a designated point. The pyrolysis vapor flowed to the LCS and condensed into liquid form. A double pipe condenser was constructed to absorb heat from pyrolysis vapor and liquified into the liquid as shown in Fig 1.

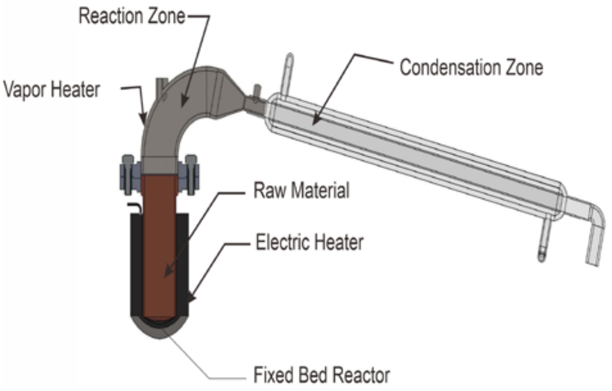

Fig. 1: Schematic process

2.3 Experimental Set-up

The ready feedstock was put in the reactor, the electric heater was on to supply heat to the reactor. The wall temperature of the reactor was controlled by a PID controller at temperature 500 ºC. The optimum reaction temperature for decomposition is 500 ºC [29] . The smaller electric heater was also installed at the wall of the reaction zone, PID also controlled it to maintain the vapor temperature at the desired operating temperature. The experimental setup schematic can be seen in **Fig 2.** Type K thermocouple was placed to investigate the system's distribution temperature, including in the reactor, reaction zone, and LCS. Table 1 shows the thermocouple's position along the pyrolysis process from the reactor to the liquid container.

Table 1. Thermocouple position

Mark	Liquid temperature
T_1	Liquid temperature
T_2	NCG temperature
T_3	Reaction zone temperature
T_4	Feedstock temperature
T_5	Inside wall temperature
T_6	Inlet condenser temperature
T_7	Inlet cooling water temperature
T_8	Outlet cooling water temperature
T_9	Ambient temperature

The data acquisition was connected to the system to record all the measurements into the computer. The vapor temperature in the reaction zone was controlled by putting the temperature sensor at the reaction zone wall, and the setting temperature varying at 150 ºC and 200 ºC and no heater (heater off). A voltage regulator and power sensor were installed to monitor the amount of electricity supplied into the reactor and reaction zone wall, and it was 1000, 1500, and 2000 Watt. The total energy supplied will affect the heating rate of the raw material. The cooling water at ambient temperature was pumped to the condenser as a cooling fluid. Hasnan at. Al. they utilized the vapor chamber to increase the cooling rate [30]. The temperature of LCS affects the total liquid yield and composition of the product. The lower boiling point of pyrolysis vapor can only liquefy during the cooling process at a lower temperature.

The product of liquid oil was collected in the measuring reservoir tank. The energy balance equations were applied to calculate the product yield as follows.

The product of liquid oil was collected in the measuring reservoir tank. The materials balance equations were applied to calculate the product yield as follows.

$$Liquid\ yield\ (\%) = (liquid\ weight)/(feedstock\ weight)\ x100\% \quad (1)$$

$$Solid\ yield\ (\%) = (Solid\ weight)/(feedstock\ weight)\ x100\% \quad (2)$$

$$Gas\ yield\ (\%) = 100\% - (liquid\ yield + solid\ yield) \quad (3)$$

The product was weighed by its mass and volume using a digital scale. The liquid outcome was characterized by its composition, heating value, viscosity, density, and pH. The product was weighed by its mass using a digital scale. The materials balance of gas yield was calculated using equation (3). The product of liquid was characterized by its composition, heating value, viscosity density, and pH.

2.4 Characterization of product

The bio-oil as a liquid product was analyzed using Gas chromatographer Agilent Technologies 7890 A and Mass spectrometry Agilent Technology 5975 C to obtain the composition and spectrometry of liquid with HP-5MS 5% Phenyl Methyl Silox, Capillary column (30 m x 250 μm x 0.25 μm). The GC oven temperature was maintained at 100 °C for 5 minutes and was programmed to increase to 260 °C at a rate of 10 °C/min for 20 minutes. The carrier gas used in the liquid product was helium gas, while methanol was used in the non-condensable gas solvent product. The calorific value was measured based on ASTM D3427 Standard and a kinematic viscosity at room temperature using ASTM D445 as standard. The compositions of liquid oil were measured for three samples: 1500 Watt with the vapor heater off, 1500 Watt, and 150 °C of vapor temperature at reaction zone as the highest liquid yield, 1500 Watt, and 200 °C. These samples will be compared to investigate the influence of vapor temperature in the reaction zone on the liquid oil composition.

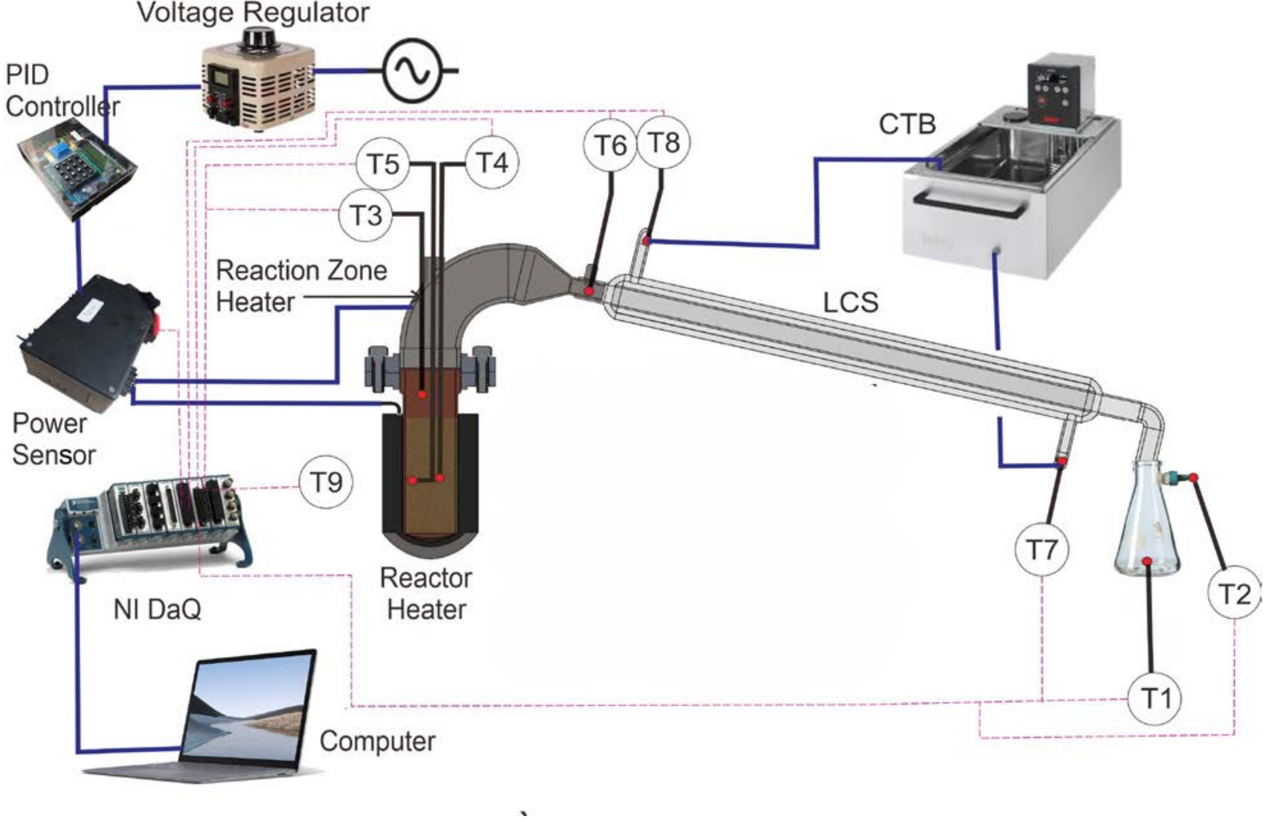

Fig. 2: Experimental setup of the pyrolysis process

3. Results and Discussion

The liquid yield and the compositions of liquid oil were influenced by vapor temperature in the reaction zone. Table 2 shows the liquid yield and other side products of pyrolysis according to the vapor temperature in the reaction zone. The maximum liquid yield was 39.0 wt%, and it was obtained at a vapor temperature of 150 ℃ with power supplied of 1500 Watt, compare to 30 wt% using nitrogen as sweep gas at low reaction temperature [18], and 63.2 wt% by flowing 25 L/minute nitrogen [19].

The maximum amount of liquid was obtained at such temperature because the reaction temperature in the reactor and the reaction zone were at the right point with the raw materials' characteristics. The higher temperature in the reaction zone will result in more gas due to the vapor's second reaction. Meanwhile, lower temperatures in the reaction zone also will produce more gases, caused by early condensation of pyrolysis vapor when reaching the wall reactor head, and this condensate falls down into the reactor. These early condensations reduce liquid yield.

The amount of power supplied to the reactor affected the heating rate and decomposition processes. The higher heating rate combined with higher vapor temperatures tended to produce more gases. The higher vapor temperature also tended to produce more gases due to the second reaction in the reaction zone. There was not any sweeping gas injected into the reactor. The pyrolysis vapor flowed into the system due to its partial pressure. The partial pressure was influenced by temperature and the molar of each component.

Table 2. The product of the pyrolysis process influenced by vapor temperature in the reaction zone

The type of feedstock	Reactor Heater (Watt)	Vapor heater ºC	Liquid (wt%)	NCG (wt%)	Char (wt%)
Biomass from *Meranti* wood	1000	Heater off	20.0	18.5	61.5
	1000	100	29.0	20.5	50.5
	1000	150	29.5%	22.0%	48.5%
	1000	200	37.0%	24.5%	38.5%
	1500	Heater off	30.0%	33.0%	37.0%
	1500	100	37.0%	25.0%	38.0%
	1500	150	39.0%	26.0%	35.0%
	1500	200	35.0%	46.5%	18.5%
	2000	Heater off	34.0%	30.0%	36.0%
	2000	100	31.5%	34.0%	34.5%
	2000	150	38.5%	30.0%	31.5%
	2000	200	35.5%	33.0%	31.5%

Fig. 3 Shows the product yield due to the vapor temperature at the reaction zone. Increasing vapor temperature more than 150 ℃ would decrease liquid yield due to the vapor cracking and second reaction. The pyrolysis process's total product using meranti wood as feedstock with the vapor temperature in the reaction zone can be seen in Fig. 4. The highest NCG was obtained at a vapor temperature of 200 °C. The reaction zone's high vapor temperature led to the vapor cracking and second reaction, and this second reaction changed the condensable gas into non-condensable gas (NCG). The Maximum char was obtained at uncontrolled vapor temperature (heater off) with electric power supplied of 1000 Watt. The effect of low heating rate and low vapor temperature at the reaction zone led to slow pyrolysis and produced more char [31].

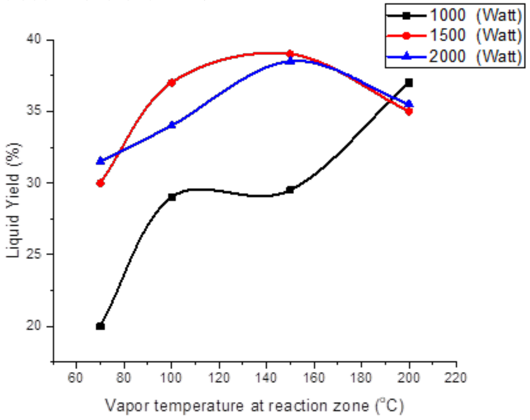

Fig. 3: The influence of vapor temperature in the reaction to the liquid yield.

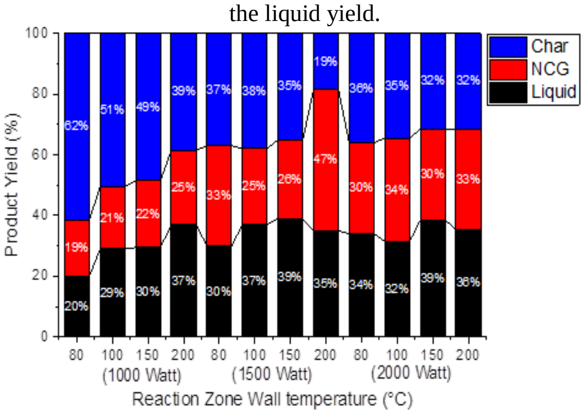

Fig. 4: The total product of the pyrolysis process using meranti wood as feedstock with the vapor temperature in the reaction zone.

The liquid yield of the pyrolysis product depends on the constituent element. The composition and compound of bio-oil were affected by many variables, such as the type of biomass, reaction temperature, vapor resident time, particle size [32], heating rate, and the feedstock's moisture content. Vapor temperature in the reaction zone also influences the composition of bio-oil. **Fig. 5** shows the GC/MS chromatographic peaks of the bio-oils. The products which were produced by varying vapor temperature have different peaks. The different product and retention times of bio-oil influenced by vapor temperature are shown in **Table 2.** Each peak represented each product, and the area of peak represents the amount of product component. There was a slight deviation peak time corresponding to the product caused by the vapor temperature.

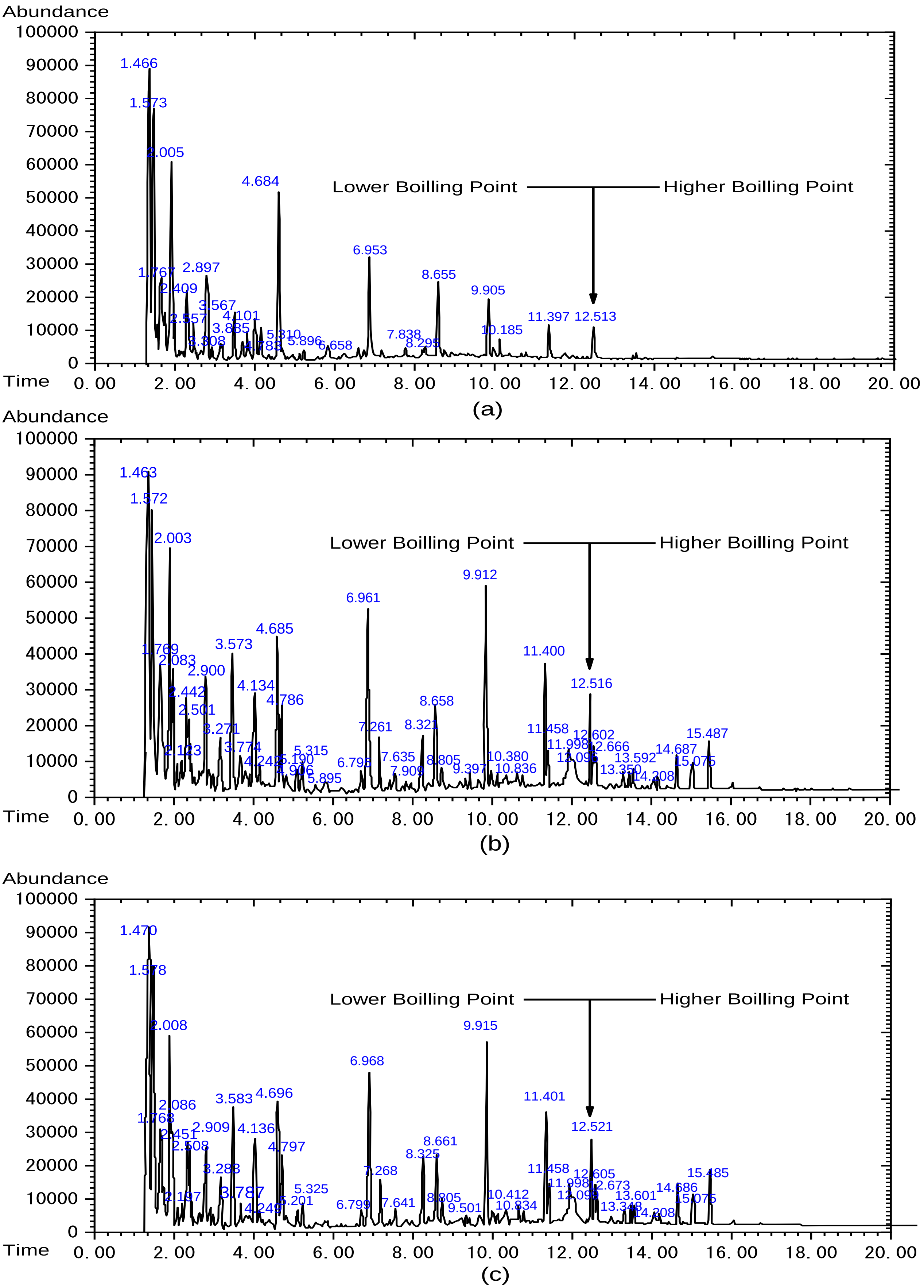

Fig. 5: GC/MS chromatographic peaks of the bio-oils collected from three samples with Maximum power supplied 1500 Watt at different vapor temperature in the reaction zone (a) Vapor Heater Off, (b) 150 °C and (c) 200 °C.

The product obtained at a vapor temperature of 150 ℃ and 200 ℃ deviated slightly from the product with the uncontrolled vapor temperature (heater off). Uncontrolled vapor temperature (heater off) had the least liquid yield and has a shorter peak (**Fig 5.a).** The peaks value were observed in 20 minutes duration, and this peak investigated the composition of the product. The uncontrolled vapor temperature was concentrated before 12.5 min. Meanwhile, vapor temperature at 150 ℃ and 200 ℃ had retention time until 15.5 min (**Fig 5.a and 5.b).** The higher vapor temperature had additional significant phenol components, acetophenone, syringyl acetone, and benzaldehyde as shown in **Table 3.** This additional component was identified as a component with a high boiling point. The element was not detected at low vapor temperature (heater off) due to the compound's high boiling point. The condensation occurred for high boiling point compounds at low-temperature exposure. There was no significant change in the composition of the substance when the vapor temperature increased from 150°C to 200 °C. The spectrum of the peak represented roughly each component corresponding to the peak. The area of each peak represented the amount of the component. The value of the peak was obtained by divided its area by a total area 33) . There was no significant difference in product between vapor temperature 150°C and 200 °C (**Fig. 5b and 5c).** There was no additional retention time peak of vapor temperature at 150°C to 200 °C. This temperature prevented the high boiling point compound from condensing in the reaction zone. There was no component at the boiling point above 200 °C.

The composition of bio-oil can be seen in **table 2**. The lower vapor temperature (heater off) produced the lower molecular weight compound than the bio-oil with higher vapor temperature. The main component of liquid oil obtained was acetic acid 20.61wt% and decreased when concentration during vapor temperature increased. The acetic acid concentration decreased to 13.62wt% and 13.54 wt% for vapor temperature 150°C to 200 °C, respectively.

Table 3. The compound and area detected from bio-oil.

No	Retention Time	Component	Area for Temperature		
			No Heater	150	200
1	1.471	Acetic acid	20.61	13.62	13.54
2	2.011	2-Cyclopenten-1-one	7.16	4.83	4.95
3	2.196	Furan, tetrahydro-2,5-dimethoxy-		0.69	0.57
4	2.500	2-Hydroxy-2-cyclopenten-1-one		1.41	2.32
5	2.619	1,3-Pentadiene, (Z)-	0.82		
6	2.837	2-Furancarboxaldehyde, 5-methyl-		0.52	
7	2.838	2-Furancarboxaldehyde, 5-methyl-	0.74		
8	2.905	Phenol	3.65		2.72
9	3.006	2(5H)-Furanone, 3-methyl-			0.59
10	3.563	2-Cyclopenten-1-one, 2-hydroxy-3-methyl-	2.45	3.21	3.47
11	3.783	2-Cyclopenten-1-one, 2,3-dimethyl-	1.37		
12	3.900	Phenol, 2-methyl-	2.16	0.68	
13	4.238	Phenol, 4-methyl-	2.03	0.68	
14	4.255	Phenol, 3-methyl-			0.62
15	4.677	Phenol, 2-methoxy-	7.29		
16	4.693	Phenol, 2-methoxy- (CAS)		3.31	3.35
17	5.138	2-Cyclopenten-1-one, 3-ethyl-2-hydroxy-	0.52		
18	5.182	4H-Pyran-4-one, 2-hydroxy-3-methyl		0.49	0.49
19	5.317	3-Ethyl-2-hydroxy-2-cyclopenten-1-one		0.73	0.71
20	5.891	Phenol, 2,4-dimethyl-	1.31	0.57	
21	6.667	Phenol, 2-methoxy-3-methyl-	0.55		
22	6.954	Creosol (Phenol, 2-methoxy-4-methyl-)	5.22	5.39	
23	6.971	1,2-Benzenediol			5.18
24	7.257	1,4:3,6-Dianhydro-.alpha.-d-glucop yranose		1.16	1.04
25	7.831	3,4-Dimethoxytoluene	0.64		
26	8.253	1,2-Benzenediol, 4-methyl-	0.63		
27	8.320	1,2-Benzenediol, 3-methoxy-	0.54	1.53	1.96
28	8.455	Hydroquinone			0.55

29	8.657	Benzeneethanol, 2-methoxy-	3.27	2.09	1.81
30	8.809	1,2-Benzenediol, 4-methyl-		0.79	0.93
31	9.737	1,4-Benzenediol, 2-methyl-		0.23	0.28
32	9.906	Phenol, 2,6-dimethoxy-	2.16	3.77	3.77
33	10.176	Phenol, 2-methoxy-4-propyl-	0.51	0.4	
34	10.412	Benzene, 2-fluoro-1,3,5-trimethyl-			0.37
35	10.699	BENZALDEHYDE, 4-HYDROXY-3-METHOXY-		0.6	0.57
36	10.834	Phenol, 2-methoxy-4-(1-propenyl)-		0.33	0.33
37	11.391	3,5-Dimethoxy-4-hydroxytoluenePhenol, 2,6-dimethoxy-4-methyl-	0.8		
38	11.407	3,5-Dimethoxy-4-hydroxytoluene		1.99	1.99
39	11.458	Phenol, 2-methoxy-4-(1-propenyl)		0.65	0.79
40	11.998	(2R,3S)-2,3-trans-3-Acetoxy-6-[(2R,3S)-2,3-trans-3-acetoxy-3',4',7,8 -tetramethoxyflavan-5-yl]-3',4',7,			2.01
41	12.099	.beta.-D-Glucopyranose, 1,6-anhydro-		1.79	2.03
42	12.504	2-(N-Methylamino)-4,5-dimethoxyani	0.77		
43	12.521	Benzocyclooctene, 7,8-dimethyl-		1.52	1.54
44	12.605	2-Propanone, 1-(4-hydroxy-3-methoxyphenyl)-		0.75	0.81
45	13.499	Phenol, 2,6-dimethoxy-4-(2-propeny l)-		0.29	0.27
46	13.601	homo - syringaldehyde			0.34
47	14.106	Phenol, 2,6-dimethoxy-4-(2-propenyl)		0.34	0.43
49	14.208	Benzaldehyde, 4-hydroxy-3,5-dimethoxy-		0.23	0.23
50	14.680	(E)-2,6-Dimethoxy-4-(prop-1-en-1-yl) phenol		0.51	0.75
51	15.068	Ethanone, 1-(4-hydroxy-3,5-dimethoxyphenyl)-		0.47	0.56
52	15.490	syringyl acetone			0.95

The vapor temperature in **Table 4** shows the caloric value and viscosity of bio-oil with different vapor temperatures. The higher heating value of 10,875 kcal/kg was obtained at a higher vapor temperature than 10,368 kcal/kg at a lower vapor temperature (heater off) due to bio-oil composition, which has a high boiling point 21) . The viscosity of liquid oil increased by increasing vapor temperature, PH, and density due to the higher molecular content of bio-oil and the high boiling point compound of bio-oil. The lower vapor temperature (heater off) was more intense to produce the lower molecular weight compound compared to the bio-oil with higher vapor temperature. The bio-oil heating value was decreased when the water content was increase 34) .

The temperature distribution during the pyrolysis process with power supplied 1500 Watt at different vapor temperatures in the reaction zone can be seen (Fig.6.a). Vapor Heater Off, (Fig.6.b) 150 °C and 200 °C (Fig.6.c). There was a vapor temperature drop during the pyrolysis process in **Fig 6. (a),** this temperature dropped due to the condensation of vapor at the reaction zone and drop to the reactor and decreased the vapor temperature at that zone. In Fig. 6 (b) and (c), the vapor temperature remained constant, and there was no vapor temperature drop due to an adequate temperature to restrict early condensation of the high boiling point compound.

Table 4. Comparison of the caloric value and viscosity of bio-oil influenced by vapor temperature

Parameter	**Units**	**Wall temperature of the reaction zone**	
		Heater off	**150 °C**
Caloric Value	Kcal/kg	10368	10875
Viscosity	cSt	1.686	1.706
Density	Gr/ml	1.229	1.280
PH		2.2	2.4

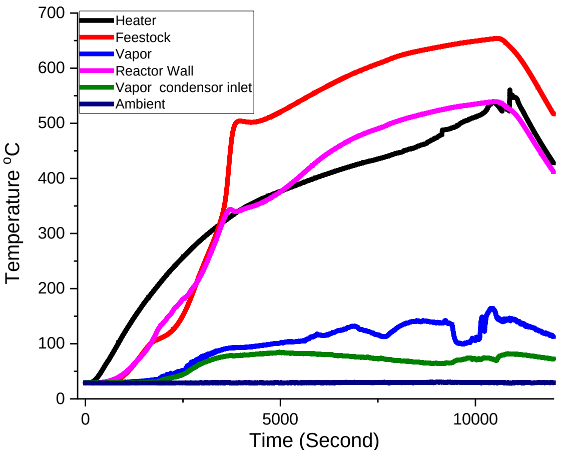

(a)

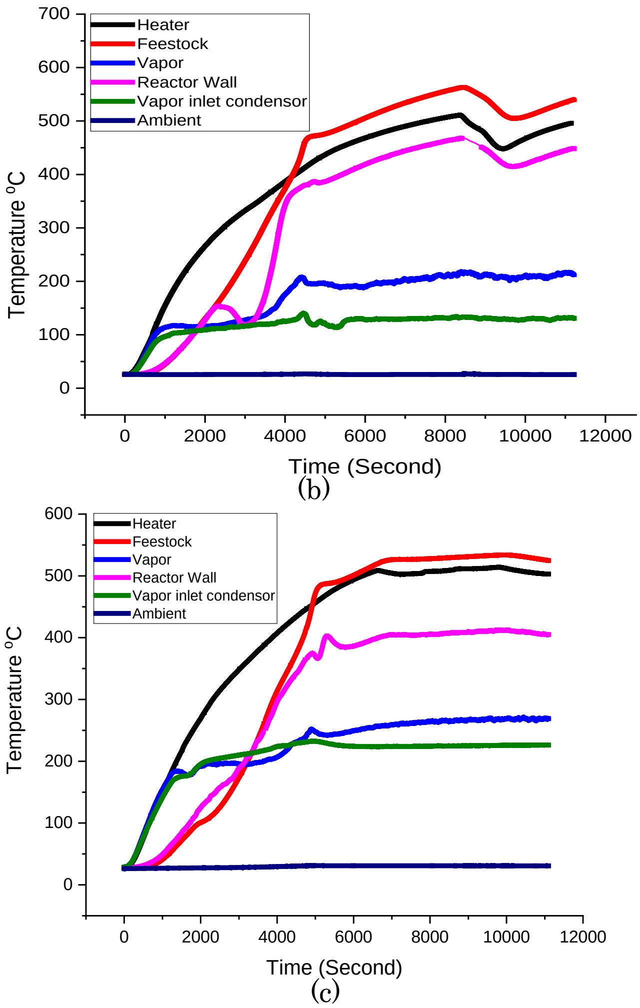

Fig. 6: Temperature distribution on the pyrolysis process with power supplied 1500 Watt at different vapor temperature in the reaction zone (a) Vapor Heater Off, (b) 150 °C and (c) 200 °C.

4. Conclusions

The non-sweep gas reactor can be applied by combining the heating at a reaction zone and obtained up to 39.0 wt% at 150 °C of vapor temperature at the reaction zone. There was no significant change in liquid oil and composition by increasing the vapor temperature until 200 °C. The higher temperature in the reaction zone would produce the bio-oil with a high boiling point substance. There was an early vapor condensation process due to the low vapor temperature, and it condensed the volatile with a high boiling compound in the reaction zone. Low vapor temperature was prevented from providing a high boiling point compound with a higher heating value. The highest heating value was obtained from 150 °C of vapor temperature. The product density increased by increasing vapor temperature. The high-density liquid had a high molecular weight of bio-oil, and it had content with a high boiling point compound. The proper temperature at the reaction zone can be applied to get the optimum liquid yield.

Acknowledgments

The authors would like to thank the DRPM (Directorate of Research and Community Service), Universitas Indonesia through the “Hibah PTUPT” scheme for funding this research.

References

1) Qu, T.; Guo, W.; Shen, L.; Xiao, J.; Zhao, K., "Experimental study of biomass pyrolysis based on three major components: hemicellulose, cellulose, and lignin," *Industrial & engineering chemistry research* **50** 10424-10433 18.(2011)
2) Furutani, Y.; Norinaga, K.; Kudo, S.; Hayashi, J.-i.; Watanabe, T., "Current situation and future scope of biomass gasification in Japan," *Evergreen: joint journal of Novel Carbon Resource Sciences & Green Asia Strategy* **4** 24-29 4.(2017)
3) Byrne, P.; Putra, N.; Maré, T.; Abdallah, N.; Lalanne, P.; Alhamid, I.; Estelle, P.; Yatim, A.; Tiffonnet, A.-L., "Design of a Solar AC System Including a PCM Storage for Sustainable Resorts in Tropical Region," *Evergreen* **6** 143-148 2.(2019)
4) Fearnside, P. M., "Global warming and tropical land-use change: greenhouse gas emissions from biomass burning, decomposition and soils in forest conversion, shifting cultivation and secondary vegetation," *Climatic change* **46** 115-158 1-2.(2000)
5) Pütün, A. E.; Apaydın, E.; Pütün, E., "Rice straw as a bio-oil source via pyrolysis and steam pyrolysis," *Energy* **29** 2171-2180 12.(2004) https://doi.org/10.1016/j.energy.2004.03.020
6) Ly, H. V.; Kim, J.; Kim, S.-S., "Pyrolysis characteristics and kinetics of palm fiber in a closed reactor," *Renewable Energy* **54** 91-95 (2013) https://doi.org/10.1016/j.renene.2012.08.053
7) Sipilä, K.; Kuoppala, E.; Fagernäs, L.; Oasmaa, A., "Characterization of biomass-based flash pyrolysis oils," *Biomass and Bioenergy* **14** 103-113 2.(1998) https://doi.org/10.1016/S0961-9534(97)10024-1
8) Ingemarsson, Å.; Nilsson, U.; Nilsson, M.; Pedersen, J. R.; Olsson, J. O., "Slow pyrolysis of spruce and pine samples studied with GC/MS and GC/FTIR/FID," *Chemosphere* **36** 2879-2889 14.(1998) https://doi.org/10.1016/S0045-6535(97)10245-4
9) Granada, E.; Míguez, J. L.; Febrero, L.; Collazo, J.; Eguía, P., "Development of an experimental technique for oil recovery during biomass pyrolysis," *Renewable Energy* **60** 179-184 (2013) https://doi.org/10.1016/j.renene.2013.05.010
10) Çağlar, A.; Demirbaş, A., "Conversion of cotton cocoon shell to hydrogen rich gaseous products by pyrolysis," *Energy Conversion and Management* **43** 489-497 4.(2002) https://doi.org/10.1016/S0196-8904(01)00037-1
11) Demirbaş, A., "Yields of hydrogen-rich gaseous

products via pyrolysis from selected biomass samples," *Fuel* **80** 1885-1891 13.(2001) https://doi.org/10.1016/S0016-2361(01)00070-9

12) Lu, M.; Lv, P.; Yuan, Z.; Li, H., "The study of bimetallic Ni–Co/cordierite catalyst for cracking of tar from biomass pyrolysis," *Renewable Energy* **60** 522-528 (2013) https://doi.org/10.1016/j.renene.2013.04.020
13) Krishna, B. B.; Biswas, B.; Ohri, P.; Kumar, J.; Singh, R.; Bhaskar, T., "Pyrolysis of Cedrus deodara saw mill shavings in hydrogen and nitrogen atmosphere for the production of bio-oil," *Renewable Energy* **98** 238-244 (2016) https://doi.org/10.1016/j.renene.2016.02.056
14) Demirbas, A.; Arin, G., "An overview of biomass pyrolysis," *Energy sources* **24** 471-482 5.(2002)
15) Bridgwater, A. V.; Meier, D.; Radlein, D., "An overview of fast pyrolysis of biomass," *Organic Geochemistry* **30** 1479-1493 12.(1999) https://doi.org/10.1016/S0146-6380(99)00120-5
16) Fang, S.; Gu, W.; Dai, M.; Xu, J.; Yu, Z.; Lin, Y.; Chen, J.; Ma, X., "A study on microwave-assisted fast co-pyrolysis of chlorella and tire in the N2 and CO2 atmospheres," *Bioresource Technology* **250** 821-827 (2018) https://doi.org/10.1016/j.biortech.2017.11.080
17) Nasruddin A Abdullah, N. P., Imansyah Ibnu Hakim, Raldi A Koestoer, "A Review of Improvements to the Liquid Collection System Used in the Pyrolysis Process for Producing Liquid Smoke," *International Journal of Technology* **8** 1197-1206 7.(2017)
18) Mazlan, M.; Uemura, Y.; Osman, N.; Yusup, S. In *Characterizations of bio-char from fast pyrolysis of Meranti wood sawdust*, Journal of Physics: Conference Series, 2015; 2015; p 7.
19) Azura, N. W.; Zularisam, A.; Norsita, S.; Nasrullah, M.; Wahida, N., "Effect of Fast Pyrolysis Operating Conditions on Product Yield of Red Meranti Sawdust," (2017)
20) Chun, Y. N.; Ji, D. W.; Yoshikawa, K., "Pyrolysis and gasification characterization of sewage sludge for high quality gas and char production," *Journal of Mechanical Science and Technology* **27** 263-272 1.(2013)
21) Schulzke, T.; Conrad, S.; Westermeyer, J., "Fractionation of flash pyrolysis condensates by staged condensation," *Biomass and Bioenergy* **95** 287-295 (2016)
22) Tripathi, M.; Sahu, J. N.; Ganesan, P., "Effect of process parameters on production of biochar from biomass waste through pyrolysis: a review," *Renewable and Sustainable Energy Reviews* **55** 467-481 (2016)
23) Heo, H. S.; Park, H. J.; Dong, J.-I.; Park, S. H.; Kim, S.; Suh, D. J.; Suh, Y.-W.; Kim, S.-S.; Park, Y.-K., "Fast pyrolysis of rice husk under different reaction conditions," *Journal of Industrial and Engineering Chemistry* **16** 27-31 1.(2010)
24) Abdullah, N. A.; Tila, J.; Hakim, I. I.; Putra, N. S. D., "An experimental study of the vapor temperature in the reaction zone for producing liquid from camphor wood in a non-sweeping gas fixed-bed pyrolysis reactor," *International Journal of Technology* **9** 1236-1245 6.(2018)
25) Supramono, D.; Lana, E. H.; Setiadi, M. N., "Effect of Carrier Gas Flow Rate on Bio-Oil Yield and Composition in Corn Cobs and Polypropylene Plastic Slow Co-Pyrolysis," *Evergreen Joint Journal of Novel Carbon Resource Sciences & Green Asia Strategy* **6** 149-156 02.(2019)
26) Supramono, D.; Edgar, J., "Characteristics of Non-Polar Bio-oil Produced by Co-pyrolysis of Corn Cobs and Polypropylene using CO_2 as Carrier Gas," *Evergreen* **6** 78-84 1.(2019)
27) Bridgwater, A. V., "Principles and practice of biomass fast pyrolysis processes for liquids," *Journal of Analytical and Applied Pyrolysis* **51** 3-22 1.(1999) https://doi.org/10.1016/S0165-2370(99)00005-4
28) Jahirul, M. I.; Rasul, M. G.; Chowdhury, A. A.; Ashwath, N., "Biofuels production through biomass pyrolysis—a technological review," *Energies* **5** 4952-5001 12.(2012)
29) Abdullah, N. A.; Novianti, A.; Hakim, I. I.; Putra, N.; Koestoer, R. A. In *Influence of temperature on conversion of plastics waste (polystyrene) to liquid oil using pyrolysis process*, IOP Conference Series: Earth and Environmental Science, 2018; IOP Publishing: 2018; p 012033.
30) Hasnan, A.; Putra, N.; Septiadi, W. N.; Ariantara, B.; Abdullah, N. A., "Vapor Chamber Utilization for Rapid Cooling in the Conventional Plastic Injection Molding Process," *International Journal of Technology* **8** 690-697 4.(2017)
31) Aguado, R.; Olazar, M.; San José, M. J.; Aguirre, G.; Bilbao, J., "Pyrolysis of sawdust in a conical spouted bed reactor. Yields and product composition," *Industrial & Engineering Chemistry Research* **39** 1925-1933 6.(2000)
32) Abdullah, N. A.; Tila, J.; Hakim, I. I.; Koestoer, R. A.; Putra, N., "Influence of Feedstock Particle Size from Merbau Wood (Intsia bijuga) on Bio-Oil Production Using a Heat Pipe Fin L-Shaped Condenser in a Pyrolysis Process," *Engineering Journal* **24** 261-271 4.(2020)
33) Ma, W.; Rajput, G.; Pan, M.; Lin, F.; Zhong, L.; Chen, G., "Pyrolysis of typical MSW components by Py-GC/MS and TG-FTIR," *Fuel* **251** 693-708 (2019)
34) Kusrini, E.; Supramono, D.; Muhammad, I. A.; Pranata, S.; Wilson, D. L.; Usman, A., "Effect of Polypropylene Plastic Waste as Co-feeding for Production of Pyrolysis Oil from Palm Empty Fruit Bunches," *Evergreen* **6** 92-97 1.(2019)